Moisture–Induced Swelling of Illinois Mine Roof Shales: A Visualized Method

Guijie Sang, Graduate Assistant
Shimin Liu, Assistant Professor
Long Fan, Phd Candidate, Mining Eng.
Pennsylvania State University
State College, PA

ABSTRACT

Weak shale roof falls have long been the main cause for fatalities in underground coal mines. Moisture-induced swelling is one of the root causes for the degradation of roof shales. In this study, slake durability tests are conducted on shale samples collected from Illinois basin coal mines, and different levels of durability are analyzed according to Gamble slake durability classification. There are two main mechanisms influencing the shape of retained fragments after two cycles of wetting and drying: mechanical abrasion and swelling pressure. A prototype optically based shale swelling apparatus is designed and manufactured for the shale free-swelling measurement. The experimental results suggest that swelling pressure tends to deteriorate shale laminations. Moisture-induced swelling of the No. 6 roof shale from Bear Run Mine was measured under 100% relative humidity condition. The measured swelling strain normal to beddings is ~5 to 7 times greater than the swelling strain parallel to beddings. This suggests that interlayer expansion plays a key role in moisture-induced swelling. Cracks induced by swelling pressure tend to occur along the bedding plane and lead to shale deterioration.

INTRODUCTION

Background

Ground falls have long been the cause for nearly 50% of all fatalities in underground coal mines and continue to be one of the greatest safety hazards in underground spaces. Among the various ground fall hazards, roof failure takes up 23% of total fatalities in underground coal mines, of which 13% are due to skin failure and 10% are due to massive roof falls (Mark, Pappas, and Barczak, 2011). Roof failures associated with weak shales are summarized in previous studies (Molinda and Mark, 2010; Aughenbaugh and Bruzewski, 1973; Bajpayee, Pappas, and Ellenberger, 2014; Murphy, 2016). For mine roof instability and failure, two aspects can explain the failure mechanism of weak roofs. One is the elevated stress concentration in lateral direction due to the mining-induced excavation and its stress redistribution around the mine opening (Song and Stankus, 1997; Fan and Liu, 2017; Hill, 1986). The other mechanism is the passive stress-relief due to the strength weakening induced by the ambient moisture and temperature fluctuations during a period of time. Shale is moisture sensitive and presents a lower durability if it is exposed to a highly humid environment for a long time, thus leading to roof deterioration and instability in underground coal mines (Aughenbaugh and Bruzewski, 1976; Stateham and Radcliffe, 1978; Chugh and Missavage, 1981; Klemetti, Oyler, and Molinda, 2009). It is well known that shale is a clay-bearing sedimentary rock and that clay minerals are water sensitive. The moisture uptake for shale will induce the micro-deformation of a shale matrix, thus the structure and strength of shale is a function of time and intensity of moisture exposure. All mine engineers notice moisture-induced shale deterioration; however, the underlying mechanism(s) are still not fully understood due to the complexity of geophysical-chemical water-shale interactions (Huang, Aughenbaugh, and Rockaway, 1986; Hensen and Smit, 2002; Diaz-Perez, Cortés-Monroy, and Roegiers, 2007). The coal mining industry is still in the process of finding a technically sound, cost-effective technology to prevent this unexpected and unpredictable shale roof failure. Therefore, understanding how the moisture-sensitive shale responses to various ambient moisture and what role exposure duration plays in shale roof failure is key to prevent unexpected roof incidents, which will lay the foundation for the long-term roof support design and ground control management.

Literature Review

The influence of water content on mechanical properties of shale has been extensively studied. Steiger and Leung (1989) shows that uniaxial compressive strength of dry shales can be 2–10 times higher than wet (native state) samples containing moisture. The results of mechanical tests on shale and clay-bearing rocks show that strength and stiffness reduce with increasing water content (Lashkaripour and Passaris, 1995; Van Eeckhout, 1976; Martin, 1966; Schmitt, Forsans, and Santarelli, 1994; Talal, 2013; Seedsman, 1987; Valès et al., 2004; Erguler and Ulusay, 2009; Vergara and Triantafyllidis, 2016). Several mechanisms for shale weakening are mentioned in the literature, attributing the reduction of strength in the presence of moisture to some potential factors, such as the following:

- reduction of fracture energy (Van Eeckhout, 1976)
- clay swelling (Huang, Aughenbaugh, and Rockaway, 1986; Sherwood and Bailey, 1994)

- frictional reduction and corrosive deterioration (Van Eeckhout, 1976; Martin, 1966)
- pore pressurization and capillary suction (Schmitt, Forsans, and Santarelli, 1994)
- ionic diffusion (Talal, 2013).

One of the main mechanisms of shale weakening is due to clay swelling. Shale contains hydrophilic clay minerals for which water shows a strong affinity. The shales imbibe the water, resulting in the clay swelling, which significantly contributes to the deterioration of shale roofs. Two types of swellings get involved accordingly: crystalline swelling due to matric suction and osmotic swelling (double layer swelling) due to osmotic suction. Matric suction results from capillary phenomenon and surface adsorption effect and is a function of moisture content, while osmotic suction is associated with the concentration of exchangeable counterions in clay-water system (Rao, Thyagaraj, and Rao, 2013).

In this study, seven types of shale samples from two coal mines located in the Illinois basin and one Marcellus outcrop are tested to determine the geomechanical properties, such as mineral composition, slake durability indices, and moisture-induced swelling. Different shales and their sensitivity to water are discussed, and mechanisms for different types of retained fragments are analyzed through slake durability tests. An optically based prototype experimental apparatus is designed to measure the time-dependent swelling due to moisture uptake. The mechanisms of swelling and the presence of cracks are also analyzed.

LABORATORY TESTS

Shale Sample Collection

The coal-bearing rocks in the Illinois Basin shown in Figure 1 are of Pennsylvanian age and were deposited dating back to about 325–290 million years ago, covering 36,800 square miles in Illinois, 6,500 square miles in southwestern Indiana, and 6,400 square miles in western Kentucky (Hatch and Affolter, 2002). The study includes the laboratory measurements on seven coal mine shale rocks collected from the Illinois basin and one Marcellus shale collected from Pennsylvania. The two coal mines are Bear Run Mine located at Carlisle, Indiana, and Wildcat Hills Mine located at Equality, Illinois (Figure 1). The Marcellus shale is collected from the outcrop of the middle Devonian Marcellus Formation at Frankstown, PA (coordinates: N40°26'00", W78°20'28"). Rock samples from the two mines were collected from actively mined areas, which are relatively fresh and well preserved at a proper temperature and humidity conditions. All collected rock samples are listed in Table 1. Bear Run Mine coal seams and roof and floor rocks are shown in Figure 2.

Mineral Composition Characterization

X-ray Diffraction (XRD) measurements were conducted for rocks A–H to characterize and quantify the mineral composition for each sample. Figure 3 shows X-ray diffraction graphs for rocks A and C. Table 2 details the major minerals distributed in the tested rocks. These results show that quartz, illite, albite, muscovite, clinochlore, and dickite make up the whole mineralogical compositions for rocks A, C, and E (No. 7, No. 6, and No. 5A roof shales) from Bear Run Mine. Rock G (Herrin No. 6) shows many different mineralogical compositions. It contains halloysite,

Table 1. Summary of the shale samples.

Location	Mine	Rock Code	Rock Type	Coal Seam
Carlisle, Indiana	Bear Run Mine (Surface Mine)	A	Roof Shale	No.7
		B	Roof Fire Clay	No.7
		C	Roof Shale	No.6
		D	Floor Shale	No.6
		E	Roof Shale	No.5A
		F	Roof Shale	No.5
Equality, Illinois	Wildcat Hills Mine (Underground Mine)	G	Roof Shale	Herrin No.6
Frankstown, PA	Marcellus Outcrops	H	Outcrop Shale	-

Figure 1. Sampling location from Illinois basin coal mines (Map is cited from [28]).

muscovite, pyrite, montmorillonite, and dolomite but contains no albite, clinochlore, or dickite. Rock D (No. 6 floor) also has different mineralogical composition compared to rock A, C, and E. It contains palygorskite, chlorite, pyrite, and calcite but contains no clinochlore or dickite. Rock B (No. 7 roof fire clay) contains a relatively high percentage of halloysite (24%), 1.2% of kaolinite, 0.2% of muscovite, and 0.2% of palygorskite. Rock F (No. 5 roof shale) contains 2.4% of pyrite and no illite. Rock H (Marcellus shale) contains 60.1% of quartz, 17.4% of illite, 3.1% Muscovite and 19.3 of phengite.

Slake Durability Test

The slake durability test (SDT) is an effective way to measure the durability of shale and clay-bearing rock samples as a function of cyclic wetting and drying and to examine the resistance to

Figure 2. Bear Run Mine coal seams and roof/floor rocks.

weakening and disintegration (Franklin and Chandra, 1972). This testing method is recommended by the International Society for Rock Mechanics (Franklin, 1979) and is standardized by the American Society for Testing and Materials. The result of slake durability test (ASTM D4644-16, 2016) for Rock Types A–H is shown in Figure 4. According to the Gamble slake durability classification (1971) shown in Table 3 and the slake durability index, after the second cycle I_{d2}, Rock D (No. 6 floor shale) and F (No. 5 roof shale) have a very high durability, with the I_{d2} up to 99.4 and 99.3, respectively. Rock A (No. 7 roof shale), E (No. 5A roof shale), G (Herrin No. 6 roof shale) and H (Marcellus outcrops) have a medium high durability. C (No. 6 roof shale) has a medium durability. B (No. 7 fire clay) has a very low durability with I_{d2} equal to zero.

Each piece of fragment collected for the SDT is intact and roughly equidimensional, following the ASTM standard. In SDT tests, retained fragments for rocks are shown in Figures 5 and 6. Experimental results show that retained fragments of rock B (fire clay) appear to be highly laminated flakes after the first cycle of wetting and drying as shown in Figure 5b. This could be attributed to the swelling pressure by water absorption. Since the laminated flakes could hardly bear any abrasion or further swelling-induced pressure, there are no retained fragments after the second cycle of ten-minute rotation in the water trough. The high percentage of halloysite and small amount of kaolinite, muscovite, and palygorskite could be the cause of the extremely low durability

Table 2. Mineralogical composition of shale samples based on XRD analysis (%).

Rock Type	Minerals	Content %	Rock Type	Minerals	Content %
No.7 Roof Shale (A)	Quartz	26.6	No.5A Roof Shale (E)	Quartz	17.3
	Illite-2M1(NR)	29.9		Illite-2M1(NR)	27.7
	Albite	9.9		Albite	3.4
	Muscovite-1M	12.3		Muscovite-1M	21.2
	Clinochlore	11.7		Clinochlore	14.7
	Dickite-2M1	9.7		Dickite-2M1	15.7
No.7 Roof Fireclay (B)	Quartz	40.6	No.5 Roof Shale (F)	Quartz	17.5
	Illite-2M1(NR)	18.6		Albite	10.9
	Dickite-2M1	15.2		Muscovite-1M	38.9
	Halloysite-14A	24		Clinochlore	24.8
	Kaolinite-2M	1.2		Dickite-2M1	5.2
	Muscovite-3T	0.2		Pyrite	2.4
	Palygorskite	0.2		Muscovite-2M1	0.3
No.6 Roof Shale (C)	Quartz	14.2	Herrin No.6 Roof Shale (G)	Quartz	22.5
	Illite-2M1(NR)	21.5		Illite-2M1(NR)	37.3
	Albite	2.7		Halloysite-14A	14.8
	Muscovite-1M	29.3		Muscovite-3T	6.3
	Clinochlore	28.9		Pyrite	4
	Dickite-2M1	3.4		Montmorillonite	11
				Dolomite	4.2
No.6 Floor Shale (D)	Quartz	24.3	Marcellus Outcrops (H)	Quartz	60.1
	Illite-2M1(NR)	29.3			
	Albite	1.2		Illite-2M2(NR)	17.4
	Muscovite-1M	8.7			
	Palygorskite	17.9		Muscovite-2M1	3.1
	Chlorite	12.6			
	Pyrite	4		Phengite	19.3
	Calcite	2			

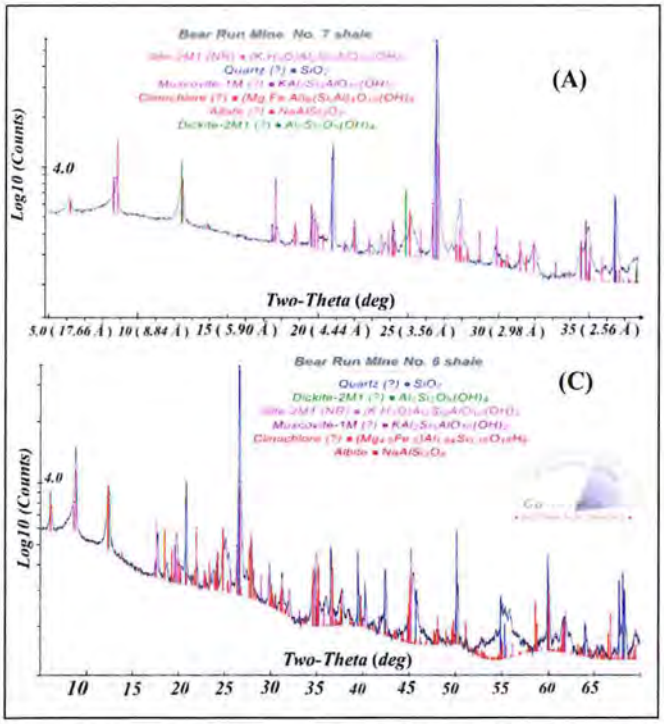

Figure 3. X-ray diffraction graphs for Rock A (Bear Run Mine No.7 Roof Shale) and Rock C (Bear Run Mine No.6 Roof Shale).

Table 3. Gamble slake durability classification.		
Group name	% Retained after One 10-min Cycle (Dry Weight Basis)	% Retained after Two 10-min Cycle (Dry Weight Basis)
Very high durability	>99	>98
High durability	98-99	95-98
Medium high durability	95-98	85-95
Medium durability	85-95	60-85
Low durability	60-85	30-60
Very low durability	<60	<30

of rock sample B (No. 7 roof fire clay). Retained fragments after the second cycle for rocks A, C, D, E, F, G, and H are shown in Figure 6. For rocks D and F, retained specimens remain virtually unchanged. While retained fragments for rocks A, C, E, G, and H contain both large and small fragments. Specifically, after two cycles of wetting and drying, retained fragments of rocks A, C, and E have round-shaped corners and flake-shaped pieces. The round-shaped corners are due to mechanical abrasion, while the flake-shaped pieces result from failure of the laminated layers due to internal swelling pressure. Retained fragments of rocks G and H have irregular shapes, containing bulky, flaky, and needle pieces, which are due to the collective effect of mechanical abrasion and swelling pressure.

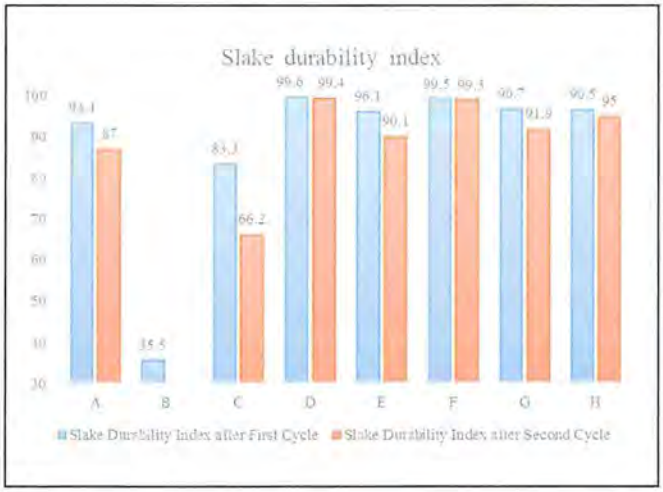

Figure 4. Slake durability index.

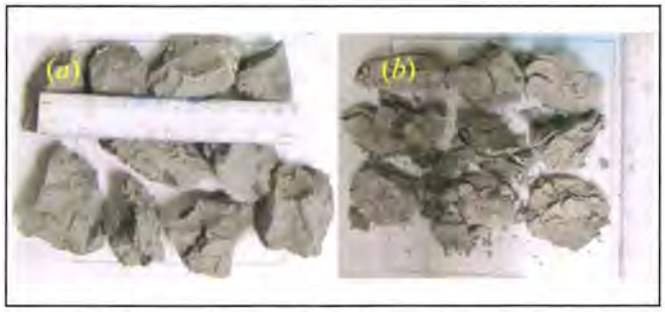

Figure 5. Slake durability test for Rock B (Fire Clay): (a) before the test; (b) after the first cycle.

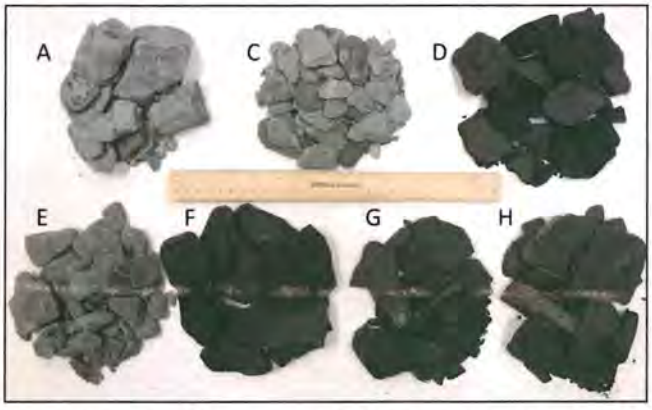

Figure 6. Retained fragments of rock A, C, D, E, F, G and H after the second cycle of SDT.

SWELLING STRAIN TEST

In the study, an optically based strain measurement apparatus is designed and manufactured for the water-vapor-induced shale swelling strain. Based on the preliminary results, the proposed optically based technique shows some advantages compared to the conventional strain-gauge-based swelling strain measurement. First, the optically based apparatus can measure much smaller samples with dimensions ranging from hundreds of micrometers

to a few millimeters, which significantly shortens the water vapor equilibrium time. With a millimeter scale shale sample, it only takes a few hours to achieve the equilibrium. Secondly, moisture-induced micro-cracks due to clay swelling could be captured by a digital microscope, which does not cause false strain due to cracking. Lastly, no water gets involved during the whole process of the specimen preparation, avoiding the pre-existing swelling strain induced by water absorption during coring, cutting, and grinding processes.

Description of Optically Based Experimental Apparatus

The optically based experiment apparatus, shown in Figure 7, includes a few subparts (from left to right):

- dry air blower consist of an air blower pump and the desiccant
- humidifier,
- moisture mixing chamber
- high-resolution digital microscope
- relative humidity meter.

The desiccant works to supply air with zero relative humidity, while the humidifier can provide water steam with 100% relative humidity. The flow rates of the air blower pump and the humidifier are both adjustable. The use of air blower pump in conjunction with the humidity meter makes it adjustable for the relative humidity in the chamber and stable at a designated value ranging from 0% to 100%. The humidity meter was placed at the outlet of the chamber to monitor and record the relative humidity and temperature.

The chamber (Figure 7) is made of a high-strength polycarbonate material with a transparent window that allows direct observation of the swelling strain during moisture absorption by the digital microscope. The sample jack inside the chamber is customized by the machine shop and is able to control the height of the sample at any level within the chamber. A thin plate with several uniformly distributed holes serves as the airflow distributor to achieve the evenly distributed airflow inside the chamber. At the middle of the base, there is a drilled hole that allows the drainage of condensed water.

Figure 7. Optically-based experimental apparatus.

The digital microscope can be handheld or mounted on a stand. The magnification range is from 20× to 220×. Different magnifications have different working distances, ranging from 4 mm to 60 mm. This is achievable through vertical movement controlled by a fine-focus adjustment knob shown in Figure 7. The adjustable horizontal arm has a 7-inch range with 360-degree rotation, and optional arm attachments are available that increase the effective range of motion. These combined features provide complete command and control of microscope orientation and positioning for maximum productivity and ease of use.

A USB cable connects the digital microscope to a computer, powering the device and providing built-in lighting. For measurements, the software, along with the digital microscope, enables the user to capture images of the object and read the actual size conveniently. Verification of the digital microscope and the software is conducted by taking a snapshot to a standard ruler shown in Figure 8. The relative error is 0.48%, which is reliable and acceptable.

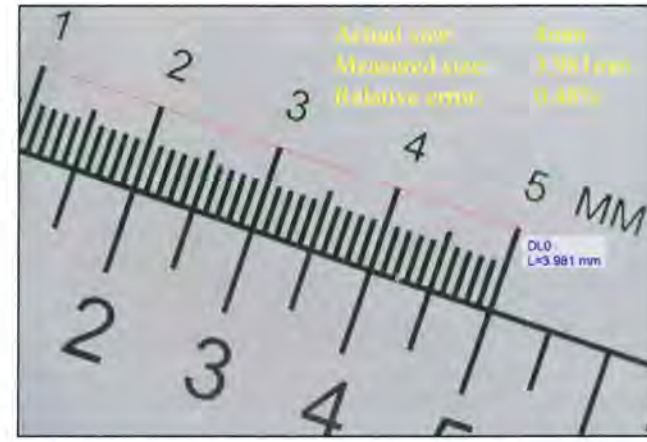

Figure 8. Verification of the digital microscope.

Shale Specimen Preparation

Four cuboid specimens (each edge is ~2 mm–8 mm) were prepared from No. 6 roof shale Bear Run Mine at Carlisle, Indiana. Each specimen was cut very carefully using a dry, slow rock saw. The cut specimen was then hand-grinded by using fine sandpapers. During the whole process of specimen preparation, there was no water involved to avoid any pre-existing swelling strain due to water absorption during coring, cutting, and grinding process. No pre-existing cracks or faults on the surfaces of four specimens were observed before the swelling tests. The four specimens were prepared from the same single piece of shale rock, which means that the four specimens had the same mineral properties. Two specimens (#1 and #2) were placed in the chamber to probe the surfaces parallel to the bedding planes, while the other two specimens (#3 and #4) were tested for the surfaces perpendicular to bedding planes. The prepared specimens are shown in Figure 9.

Measurements of Swelling Strain With Continuous Water Moisture Uptake

Time-dependent swelling of specimens (No. 6 roof shale) under 100% relative humidity was continuously monitored by the optically based experiment apparatus. Images were captured by the digital microscope to measure the areal strain for specimens #1 and #2 and linear strain for specimens #3 and #4. Since surfaces of the specimens are not perfect rectangles, the polygon measurement feature was used to measure the areal changes parallel to the bedding planes for specimens #1 and #2 (Figure 10a and b), while linear deformations normal to beddings were measured for specimens #3 and #4 (Figure 10c and d).

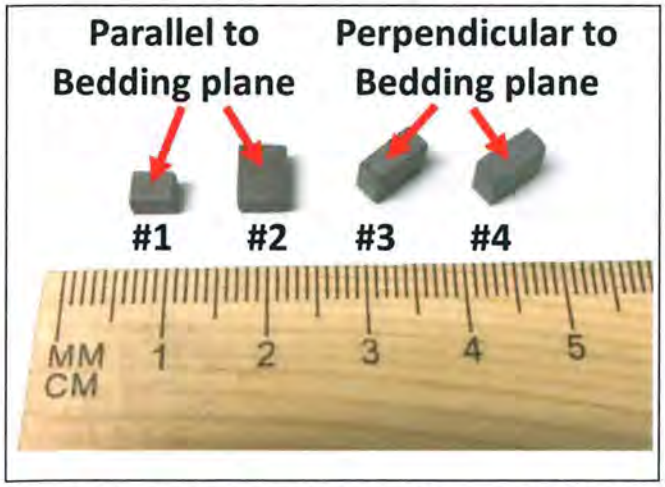

Figure 9. Four specimens (No.6 roof shale) prepared for the test.

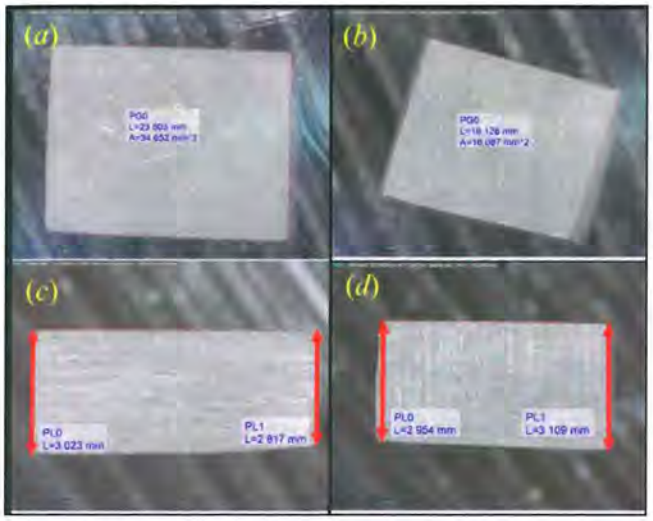

Figure 10. Snapshot by digital microscope and measurement of dimension: (a) specimen #1, (b) specimen #2, (c) specimen #3, (d) specimen #4.

Areal strain is defined as the change in the plane surface area divided by its original area (A) with its dimension of $a \times b$.

$$\varepsilon_s = \frac{\Delta A}{A} = \frac{(a+\Delta a)(b+\Delta b) - ab}{ab} \cong \frac{\Delta a}{a} + \frac{\Delta b}{b} = \varepsilon_a + \varepsilon_b \qquad (1)$$

Assuming the surface parallel to the bedding plane is isotropic, according to the equation above, the linear strains parallel to the bedding planes for specimens #1 and #2 are $\varepsilon_l = \varepsilon_a = \varepsilon_b = \varepsilon_s/2$.

The linear strains (ε_n) normal to bedding plane for specimens #3 and #4 are defined as the change in normal length of the sample divided by its original normal length. Two edges normal to bedding plane were measured to obtain an average value, defining the linear strain normal to bedding plane.

Experimental Measured Strain Results and Discussion

Figures 11 and 12 show the results of linear strains parallel and normal to beddings. Swelling strains under 100% relative humidity come to 5.0% (#1) and 3.4% (#2), 25.1% (#3) and 22.5% (#4). These results suggest a strong swelling potential for the No. 6 roof shale subject to water vapor uptake. The uptake of water vapor into shales, either by matric suction or by osmotic suction, results in the net matrix swelling strain. From the results, it was found that the final equilibrium can only be achieved in hundreds of minutes. This short equilibrium time is attributed to the high ratio of surface area to volume for this study, which allows the fast equilibrium diffusion in the sample. This is an advantage for the optically based measurement since the traditional shale core swelling strain is measured on large specimens using strain gauge, which takes an extensive amount of time to achieve the final equilibrium.

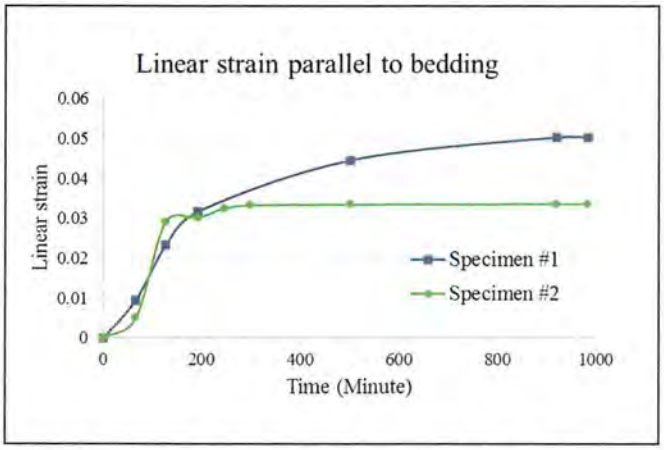

Figure 11. Linear strain parallel to bedding for specimens #1 and #2.

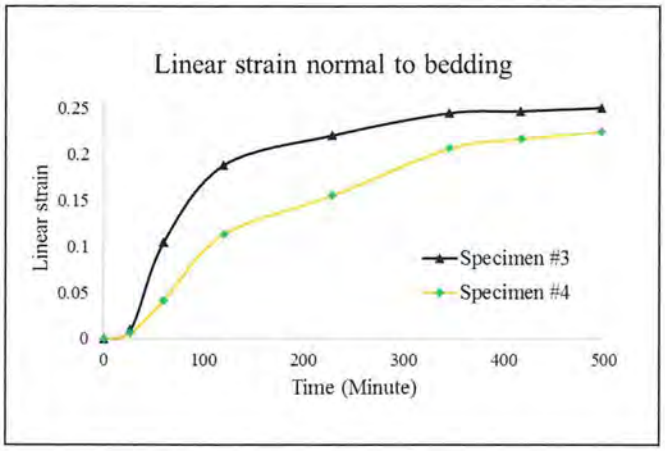

Figure 12. Linear strain normal to bedding for specimen #3 and #4.

As expected, the swelling strain normal to beddings is ~5–7 times greater than the swelling strain parallel to beddings, suggesting that the interlayer expansion plays a key role in the moisture-induced swelling. This can also lead to shale deterioration along the bedding plane (Figure 13). Specifically, no cracks were

observed on surfaces parallel to beddings for all the specimens. As shown in Figure 13, however, water-absorption-induced cracks were observed on the surface normal to beddings for specimen #3 after 60 minutes and #4 after 228 minutes. Since the swelling measurements are conducted under unconfined conditions, the effect of the mechanical abrasion involved during the slake durability test can be excluded. Therefore, the effect of swelling pressure on unconfined shale samples contributes exclusively to the crack initiation and propagation.

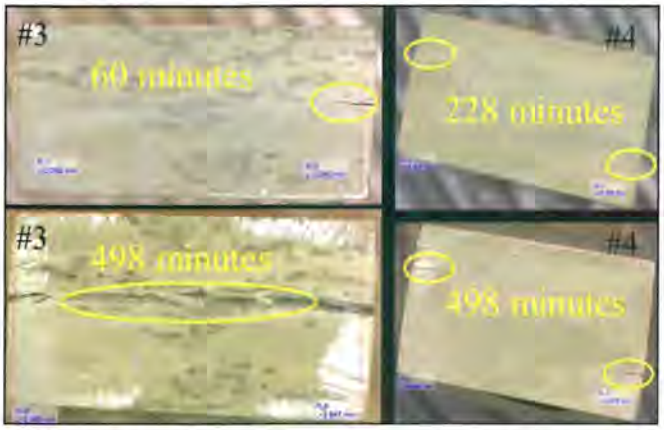

Figure 13. Moisture-induced cracks along bedding plane observed on the surface of specimen #3 and #4.

DESIGN CONSIDERATIONS

Deterioration of roof shales occur over time and may induce roof falls in underground coal mines due to the weathering behavior of weak roof shales and their moisture sensitivity. Some means were employed for underground coal mines in Illinois basin to avoid roof falls and maintain a long-term roof stability such as installation of humidity monitoring and controlling systems, coated protection with sealant, installation of roof screens and roof bolts and so on.

Typical roof falls in underground mines can be summarized as three types based on the destructiveness: skin failure between anchor points, roof fall without bolt failure and roof fall with bolt failure.

As the shale roofs contain laminated layers, the cracks could occur along the bedding planes in humid environment, causing the layer separation within shale mass. The possible consequence could be skin failure at non anchorage zone. In this case, it is recommended to cut the contact between shales and air as soon as possible after caving. For example, using artificial sealant to protect the roof shale from moisture, such as shotcrete, gunite, tar and polymeric (Gurgenli, 2006), or installing wire mesh at crucial positions. Also, leaving thin roof coal as a sealant is proposed by engineers. This solution, however, still takes the risk of roof coal fall.

At the location where the roof bolts are not fully grouted with resin or concrete, roof fall without bolt failure sometimes occur. Since moisture in the air could migrate along the hole of roof bolt system, moisture could easily penetrate through bolted interval and deteriorate weathered strata beyond anchorage zone, leaving the height of roof fall equals to the bolt length. Therefore, the installation of fully grouted roof bolts can reinforce weak roofs much more efficiently. Besides, another effective way is to install longer roof bolts or cable bolts, since longer supports are able to anchor in stronger rock strata.

As it is discussed in the swelling strain test section, the maximum moisture-induced shale strain could be as much as 25.1%, which indicates a strong swelling potential of shale and its high sensitivity to moisture. This experiment is conducted under unconfined condition and it demonstrates the obvious swelling in the direction perpendicular to beddings. However, in most cases, the deformation of roof shale is always confined by bolts. Instead of swelling along the bolt, the moisture-induced swelling will passively increase the anchor force supplied by the bolt, which can easily cause the failure of the bolt and consequently lead to sever roof falling accidents. In this situation, a relative small anchor force is recommended in order to offer more capacity to release the moisture-induced swelling stress. The selection of anchor force is crucial to support design. Too small anchor force cannot fully exert considerable influence within the roof.

Before making a final support design, engineers should acquire the basic test data of shale roof, such as the UCS, BTS, PLT, slake durability and moisture-induced swelling strain test. If the initial strength of shale roof is very weak or/and the moisture has a significant influence on its strength, there will be a great chance that the bolt only strengthens the rock in a limited region due to the difficulty in constructing the force anchor within weak roof. Increasing the bolts density should be considered according to the basic mechanical tests and moisture-strain test of roof shale. The experimental study in this paper is able to offer the fundamental information for roof control and support design. However, more information should be acquired in order to optimize the long-term roof support design. Besides, to characterize the stress evolution and time effect of shale sample under confined condition with the influence of moisture also plays a key role for the long-term roof support design and roof control.

SUMMARY AND CONCLUSION

From the preliminary laboratory measurements and analyses, some main conclusions and summaries are as follows:

1. The slake durability test is an effective way to test shale resistance to weakening and disintegration and to examine mechanisms of disintegration. The higher the SDT index, the higher the durability. The shapes of retained fragments are influenced by both mechanical abrasion and swelling pressure. Swelling pressure tends to fail the specimen along the laminations.
2. The optically based swelling apparatus is designed and manufactured to measure the water-absorption-induced shale strain. It is effective and straightforward and only requires hundreds of minutes to achieve the final equilibrium condition.
3. Swelling strain normal to beddings is ~5–7 times greater than the swelling strain parallel to beddings, concluding that the interlayer expansion plays a key role in the moisture-induced swelling.
4. Cracks induced by swelling pressure occur along the bedding plane for the No. 6 roof shale under 100% relative humidity, leading to shale weakening and deterioration.

ACKNOWLEDGEMENT

This work was financially supported by The National Institute of Occupational Safety and Health (NIOSH) under the contract No. NIOSH-200-2016-90385. The authors would like to acknowledge our coal mine partners for the mine access and rock sampling.

REFERENCES

ASTM D4644-16. (2016). Standard Test Method for Slake Durability of Shales and Other Similar Weak Rocks. West Conshohocken, PA: ASTM International. https://www.astm.org/Standards/D4644.htm

Aughenbaugh, N. B. and Bruzewski, R. (1973). *Investigation of the Failure of Roofs in Coal Mines*. Washinton DC: U.S. Department of the Interior, Bureau of Mines.

Aughenbaugh, N. and Bruzewski, R. (1976). *Humidity Effects on Coal Mine Roof Stability*. Final Contract Report. Pittsburgh, PA: National Institute for Occupational Safety and Health. NIOSHTIC No. 10000918, pp. 164.

Bajpayee, T., Pappas, D. M., and Ellenberger, J. L. (2014). "Roof instability: What reportable noninjury roof falls in underground coal mines can tell us." *Professional Safety* 59(3): 57–62.

Chugh, Y. P. and Missavage, R. A. (1981). "Effects of moisture on strata control in coal mines." *Engineering Geology* 17(4): 241–255.

Diaz-Perez, A., Cortés-Monroy, I., and Roegiers J. (2007). "The role of water/clay interaction in the shale characterization." *Journal of Petroleum Science and Engineering* 58(1–2): 83–98.

Erguler, Z. and Ulusay, R. (2009). "Water-induced variations in mechanical properties of clay-bearing rocks." International Journal of Rock Mechanics and Mining Sciences 46(2): 355–370.

Fan, L. and Liu, S. (2017). "A conceptual model to characterize and model compaction behavior and permeability evolution of broken rock mass in coal mine gobs." *International Journal of Coal Geology* 172: 60–70.

Franklin, J. and Chandra, R. (1972). "The slake-durability test." *International Journal of Rock Mechanics and Mining Sciences & Geomechanics Abstracts* 9(3): 325–328.

Franklin, J. A. (1979). Suggested methods for determining water content, porosity, density, absorption and related properties and swelling and slake-durability index properties. *International Journal of Rock Mechanics and Mining Sciences & Geomechanics Abstracts*, 16(2): 141-156.

Gamble, J. C. (1971). *Durability-Plasticity Classification of Shales and Other Argillaceous Rocks*. Doctoral Thesis. Champaign, IL: University of Illinois at Urbana-Champaign.

Hatch, J. R. and Affolter, R. H. (2002). "Resource assessment of the Springfield, Herrin, Danville, and Baker coals in the Illinois Basin." USGS Fact Sheet 072-02. Reston, VA: U.S. Geological Survey, pp. 4.

Hensen, E. J. and Smit B. (2002). "Why clays swell." *Journal of Physical Chemistry* 106(49): 12664–12667.

Hill, J. L. (1986). *Cutter Roof Failure: An Overview of the Causes and Methods for Control*. Washington, DC: U.S. Department of the Interior, Bureau of Mines. Information Circular 9094, pp. 44.

Huang, S., Aughenbaugh, N., and Rockaway, J. (1986). "Swelling pressure studies of shales." *International Journal of Rock Mechanics and Mining Sciences & Geomechanics Abstracts* 23(5): 371–377.

Klemetti, T., Oyler. D., and Molinda, G. (2009). "Time-dependent roof deterioration at a central Ohio coal mine." In: *Proceedings of the 28th International Conference on Ground Control in Mining*. Morgantown, WV: West Virginia University, pp. 248–255.

Lashkaripour, G. and Passaris, E. (1995). Correlations between index parameters and mechanical properties of shales. In: *Proceedings of the 8th ISRM Congress*. Lisbon, Portugal: International Society for Rock Mechanics.

Mark, C., Pappas, D., and Barczak, T. (2011). "Current trends in reducing ground fall accidents in US coal mines." *Mining Engineering 63*(1): 60–65.

Martin, R. A. (1966). *The Effect of Moisture on the Compressive and Tensile Strength on a Variety of Rock Materials*. Master Thesis. Rolla, MO: Missouri University of Science and Technology, pp. 134.

Molinda, G. and Mark, C. (2010). "Ground failures in coal mines with weak roof." Electronic Journal of *Geotechnical Engineering 15*(F): 547–588.

Murphy, M. (2016). "Shale failure mechanics and intervention measures in underground coal mines: Results from 50 years of ground control safety research." *Rock Mechanics and Rock Engineering 49*(2): 661–671.

Rao, S. M., Thyagaraj, T., and Rao, P. R. (2013). "Crystalline and osmotic swelling of an expansive clay inundated with sodium chloride solutions." *Geotechnical and Geological Engineering 31*(4): 1399–1404.

Schmitt, L. Forsans, T., and Santarelli, F. (1994). "Shale testing and capillary phenomena." *International Journal of Rock Mechanics and Mining Sciences & Geomechanics Abstracts 31*(5): 411–427.

Seedsman, R. (1987). "Strength implications of the crystalline and osmotic swelling of clays in shales." *International Journal of Rock Mechanics and Mining Sciences & Geomechanics Abstracts 24*(6): 357–363.

PROCEEDINGS OF THE 36th International Conference ON GROUND CONTROL IN MINING

Edited by

Brijes Mishra | Heather Lawson | Michael Murphy | Kyle Perry

Published by the
Society for Mining, Metallurgy & Exploration

Society for Mining, Metallurgy & Exploration (SME)
12999 E. Adam Aircraft Circle
Englewood, Colorado, USA 80112
(303) 948-4200 / (800) 763-3132
www.smenet.org

The Society for Mining, Metallurgy & Exploration (SME) is a professional society whose more than 15,000 members represents all professionals serving the minerals industry in more than 100 countries. SME members include engineers, geologists, metallurgists, educators, students and researchers. SME advances the worldwide mining and underground construction community through information exchange and professional development.

Information contained in this work has been obtained by SME from sources believed to be reliable. However, neither SME nor its authors and editors guarantee the accuracy or completeness of any information published herein, and neither SME nor its authors and editors shall be responsible for any errors, omissions, or damages arising out of use of this information. This work is published with the understanding that SME and its authors and editors are supplying information but are not attempting to render engineering or other professional services. Any statement or views presented herein are those of individual authors and editors and are not necessarily those of SME. The mention of trade names for commercial products does not imply the approval or endorsement of SME.

ISBN 978-0-87335-456-1